Nuclear Instruments and Methods in Physics Research A 680 (2012) 90–96

Contents lists available at SciVerse ScienceDirect

Nuclear Instruments and Methods in Physics Research A

journal homepage: www.elsevier.com/locate/nima

A high speed digital data acquisition system for the Indian National Gamma Array at Tata Institute of Fundamental Research

R. Palit [a,*], S. Saha [a], J. Sethi [a], T. Trivedi [a], S. Sharma [a], B.S. Naidu [a], S. Jadhav [a], R. Donthi [a], P.B. Chavan [a], H. Tan [b], W. Hennig [b]

[a] Tata Institute of Fundamental Research, Colaba, Mumbai 400 005, India
[b] XIA LLC, Hayward, CA 94544, USA

ARTICLE INFO

Article history:
Received 20 November 2011
Accepted 28 March 2012
Available online 5 April 2012

Keywords:
Gamma ray spectroscopy
Nuclear structure
Digital data acquisition system

ABSTRACT

A digital data acquisition system for the Compton suppressed clover detector array has been implemented at the TIFR-BARC accelerator facility for the high resolution gamma ray spectroscopy using the Pixie-16 Digital Gamma Finder modules by XIA LLC. This system has a provision for simultaneous digitization of 96 preamplifier signals of high purity germanium crystals. The energy and timing characteristics of the clover detectors have been investigated in detail. In-beam data has been collected both in singles and in the coincidence mode. The system has been tested with 64 channels with each of the 64 crystals having an event rate up to 5 kHz and 2-fold clover coincidence rate up to 15 kHz. The use of the digital data acquisition system has improved the high counting rate handling capabilities for the clover array. Conventional systems with analog shaping are being replaced by digital system that provides higher throughput, better energy resolution and better stability for the multi-detector Compton suppressed clover array.

1. Introduction

A basic property of the nucleus is its geometrical shape which is the result of the delicate balance between the shell structure and the residual interactions between the nucleons. Discrete gamma ray spectroscopy using large array of Compton suppressed high purity germanium detectors, e.g., Gammasphere [1], Clarion [2], Clara [3], Yrast ball [4], GASP [5], Exogam [6], Rising [7], Afrodite [8], Tigress [9], Greta [10], Grape [11], Jurogam [12], and INGA [13] continues to provide new insights on the symmetry of the nuclear mean field and the residual interactions among the nucleons. A collaborative research facility called the Indian National Gamma Array (INGA) was initiated by Tata Institute of Fundamental Research, Inter University Accelerator Center, Bhabha Atomic Research Centre, Saha Institute of Nuclear Physics, Variable Energy Cyclotron Centre, UGC-DAE-Consortium for Scientific Research, and many Universities in India [13]. This array (INGA) consisting of Compton suppressed clover detectors facilitates polarization and lifetime measurements for the excited states due to the segmented structure of clovers and its higher efficiency [14,15]. INGA along with other ancillary detectors using analogue electronics and CAMAC based data acquisition system has been used for the investigation of variety of nuclear structure phenomena, e.g., shape coexistence, magnetic/anti-magnetic rotation, chiral rotations, coupling of gamma vibration with other modes, high spin states of neutron rich nuclei in sd-shell, and isomers near shell closure [16–21]. Recently, a PCI-PXI based digital data acquisition (DDAQ) system with 96 channels has been implemented for the Compton suppressed clover array. In this paper, we present the specifications for the digital data acquisition system for the array to be used for the in-beam experiments, the basic architecture, the coincidence event building from the time-stamped data, the energy and timing characteristics of the clover detectors, the Compton suppression of the clovers using logic inputs to the Pixie-16 modules and performance of the system at high count rate [22,23]. The results from the commissioning in-beam experiment of the complete set-up and scope for the future nuclear structure and reaction measurements are mentioned in this paper.

2. Basic feature of the clovers and Compton suppressed BGO shields of the array and the requirements of the associated DDAQ

The Compton suppressed clover detectors used in the present array are discussed in detail in Refs. [24,25]. Each of the clovers has four n-type crystals kept in a single cryostat. Each crystal is connected to a low temperature FET coupled with the resistive charge sensitive preamplifier. The preamplifier has a gain of

* Corresponding author. Tel.: +91 22 2278 2562; fax: +91 22 2280 4610.
E-mail address: palit@tifr.res.in (R. Palit).

0168-9002/$ - see front matter © 2012 Elsevier B.V. All rights reserved.
http://dx.doi.org/10.1016/j.nima.2012.03.046

200 mV/MeV and the decay time constant of the output is 50 μs. The Compton suppressed BGO shield has 16 photomultiplier and operates at 950 V. The sum of the 16 photomultipliers is given to a timing filtering amplifier and then to the analogue constant fraction module which generates a NIM logic signal. This goes as an input to the digital data acquisition system for the veto of the clover signals. The detector array is designed for 24 Compton suppressed clover detectors arranged in a spherical geometry with six detectors at 90° and three detectors each at 23°, 40°, 65°, 115°, 140° and 157° with respect to the beam direction [26]. The distance from the target to crystal is 25 cm and the overall photopeak efficiency is around 5% at $E_\gamma \sim 1$ MeV.

The requirements of the TIFR digital DAQ is to provide the energy and timing information for all the 96 channels of 24 clovers vetoed with the respective Compton suppressed BGO shields. The system should be able to handle high count rate (20 kHz) for each crystal without deteriorating the energy resolution over the full dynamic range of the clovers. The timing properties of each of the crystals should be optimized with the digital system so that lifetime measurements for the isomers should also be possible with pulsed beam experiments. The system should have the capability to provide low-fold as well as high-fold coincidence data for in-beam experiments. Low-fold coincidence data with the large array in coincidence with the charged particle detection will be quite useful for investigation of non-yrast states of nuclei populated through direct reaction channels. For nuclear reaction cross-section measurements using on-line gamma measurements it is highly desirable to operate the system with a zero dead time [27]. Coupling the clover detector data acquisition system with other ancillary detectors like NaI(Tl) gamma-ray multiplicity filter, $LaBr_3$(Ce) fast timing detectors and CsI(Tl), Si charged particle detectors is also required. The present system consisting of the Pixie-16 modules with PCI-PXI based architect meets the aforementioned requirements and seems to be a very effective for yrast and near yrast spectroscopy of exotic isotopes.

3. Basic configuration of the DDAQ

The DDAQ has six Pixie-16 modules, two LVDS level translator modules, and one controller arranged in a single CompactPCI/PXI crate. The crate is connected to the windows PC via a MXI-4 PXI-PCI optical bridge. Each Pixie-16 card has 16 channels and serves to four clover detectors. The block diagram of the system is shown in Fig. 1. Elaborate technical information about digitizer Pixie-16 modules can be found in Ref. [22]. Only, the complex triggering capability of the Pixie-16 modules adopted for the present experimental set-up will be briefly described in the following.

The clover produces four signals from the core of the four crystals. Therefore, each Pixie-16 card supports four clover detectors. The preamplifier signal is digitized with a 12-bit 100 MHz Flash Analog to Digital Converter (FADC). The digitized data stream of the incoming analog pulse enters the signal processing circuitry. This generates a trigger through a fast filter for total multiplicity computation in the on-board FPGA. The fast trigger is generated when the fast trapezoid filter output crosses the defined threshold. The fast triggers generated from any of the 16 channels of a Pixie-16 module can be distributed to its adjacent modules through the PXI backplane for generation of global trigger. In the present configuration, of the six cards in a single crate one card named as Director receives and distributes the triggers among all the channels. The Director computes the multiplicity and opens the coincidence window with a defined length. The veto signal of the BGO shield is given via the front panel LVDS I/O port. A valid fast trigger is generated in absence of the veto pulse in a specific

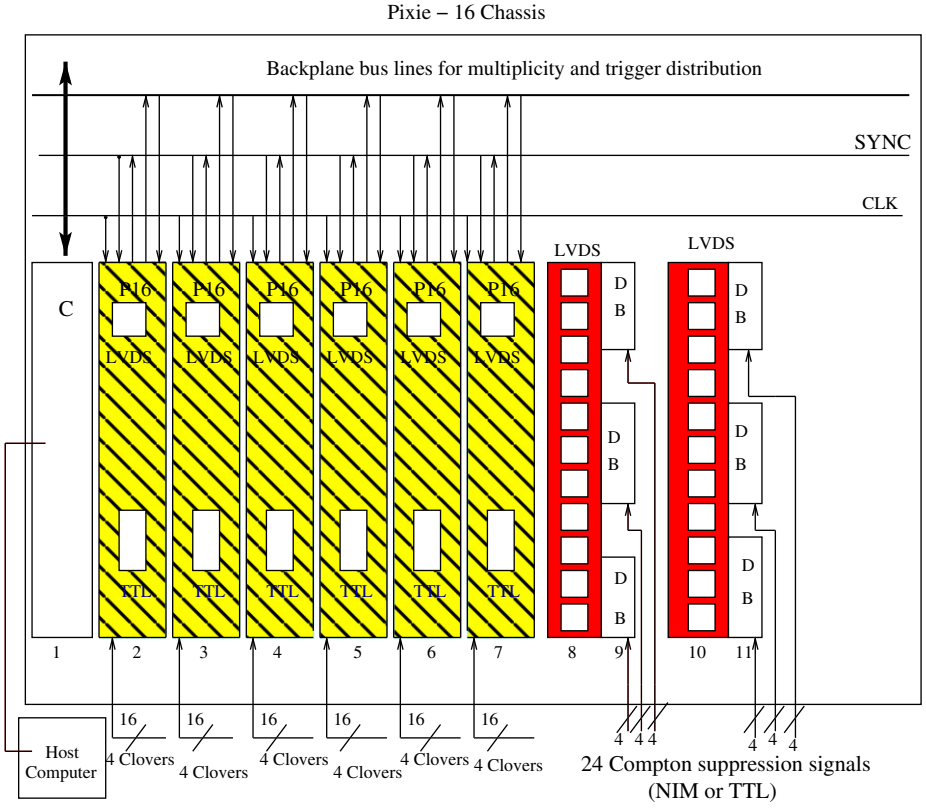

Fig. 1. Block diagram for the digital DAQ for 24 Compton suppressed clover detectors. It has six Pixie-16 modules, two LVDS level translator modules and one controller arranged in a single CompactPCI/PXI crate.

time window. For a given channel the fast trigger validated by the external trigger and not vetoed by channel veto signal, the time-stamp will be latched and the event header information will be written. All the modules are required to synchronize clocks for the coincidence measurement.

4. Generation of one and higher dimensional spectra from the time-stamped data

The PC monitors the status of the FIFOs of each module in the crate through the MXI-4 optical bridge. Once the FIFO is ready the data is transferred to the PC in block mode and written to the respective file of the module. The full data stream is written to six files for the current configuration which are opened and closed in the beginning and end of each run, simultaneously. First, the time-stamped data from different modules are merged to a single data stream as per the 48 bit 100 MHz time-stamp and event number. The event building software "Multi pARameter time-stamped based COincidence Search program (MARCOS)" written at TIFR sorts the combined data stream to usual coincident events based on the mapping of DDAQ channels to different crystals of the detectors. A typical spectrum showing the time difference between the consecutive events from the combined data stream of all the four module is shown in Fig. 2. The initial portion of the spectrum shown in the inset represents the prompt coincident events followed by the random and delayed components. The gains of the different crystals have been matched by the event building program by energy calibration coefficients. The event building program has the capability of making prompt gamma—prompt gamma correlations as well as the prompt gamma—delayed gamma correlation study by choosing the proper time windows as the external parameters. Conditional time spectra are also generated to look for the prompt and delayed components between different transitions.

5. Performance from radioactive source test and in-beam experiments

The performance of the present DDAQ system has been characterized with a number of test experiments with the source as well as in-beam experiments. In the following the detailed results are presented.

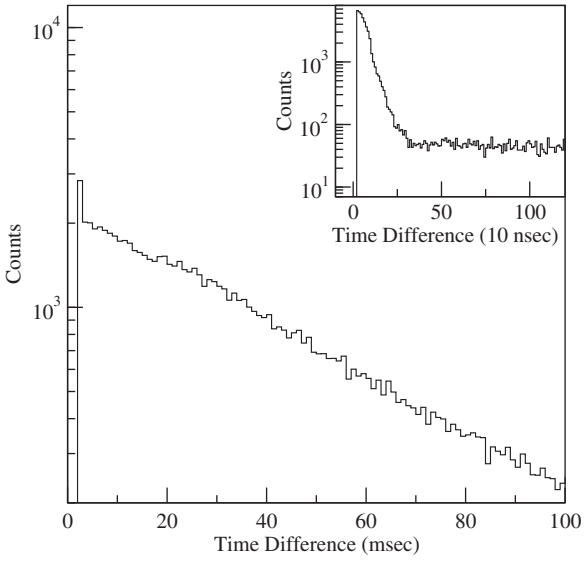

Fig. 2. Time difference between the consecutive events. The inset shows the expanded portion of the spectrum for smaller time difference and the peak near the zero channel corresponds to the coincidence events.

5.1. Energy resolution, addback of clover and the Compton suppression

The energy calibration was carried out with the different known transitions of ^{152}Eu and ^{133}Ba radioactive sources. The coefficient of the quadratic term is around 2×10^{-8}. Usually, a given experiment continues for 5 days and the gain of each channel is required to be constant over this period. Due to less number of active components the present system provides a stable gain for all the channels in the experiment. The energy resolution of the 1332 keV transition of ^{60}Co is about 0.16% for a typical crystal of the clover with 1000 counts/s. After gain matching all the crystals of a clover, event wise addition of energy generates the addback spectrum with energy resolution of about 0.18% for the same energy. The number of counts in the 1333 keV peak becomes 1.44 times large in the addback mode. Similar energy measurement was carried out by moving the ^{60}Co source from the target position in the array towards the detector. With the increasing count rate the energy resolution deteriorates by 0.01% at 20 kHz count rate. Previous readout systems of INGA based on analog electronics have limitations due to long term temperature induced gain drift and in-ability to keep up with high count rates. The new DDAQ of the INGA clearly overcomes these limitations of the previous analogue system.

The sum signal of the 16 PMTs of the BGO Compton shield was fed to a TFA and CFD combination to generate a NIM logic signal. The output of the CFD was kept around 100 ns. The threshold of the BGO was chosen to be around 40 keV in the CFD. This Compton shield CFD signal was fed to the NIM to LVDS fan-out module kept in the PXI crate. Each of these NIM to LVDS fan-out modules have 12 channels. Two such modules were used for the Compton suppression of 24 clovers. The LVDS veto signal was sent to the Pixie-16 through its front panel LVDS I/O port. Through the front panel digital I/O port, the veto signal is watched on the fast digital scope to adjust the delay with the first filter output of the crystals of the clovers. The first filter was delayed by 200 ns with respect to the start of the veto signal. A peak-to-total in the spectrum for a ^{60}Co source at the target position with addback for the unbiased and biased shields were measured to be around 22% and 40%, respectively. These ratios are comparable to our previous measurements using analogue electronics.

5.2. Timing measurements

The preamplifier pulses for 1333 keV transition as measured with the Pixie-16 for one of the crystals of a clover are depicted in Fig. 3(a). Due to larger crystal size the rise time of the pulses varies from 100 to 300 ns for 1333 keV photopeak. To understand the timing properties of the clover, coincidence measurement was set up using a BaF_2 crystal and one crystal of the clover. The ^{60}Co was used for the coincidence measurement. The BaF_2 signal was given to analogue CFD and the threshold was kept as high as 1 MeV. The logic signal from the CFD was given to a pulser which generates a signal with an exponential decay time about 1 μs. Leading edge trigger in the fast filter was used to get the timing resolution between the BaF_2 and the clover crystal. The timing peak was found to have a rms of 10 ns for the coincidence between 1172 and 1333 keV transitions. For further improvement of the timing properties, the traces of the HPGe pulses were stored with a trace-length of 2 μs. First the fast filter response of the digitized waveform Trace[i] is computed using the

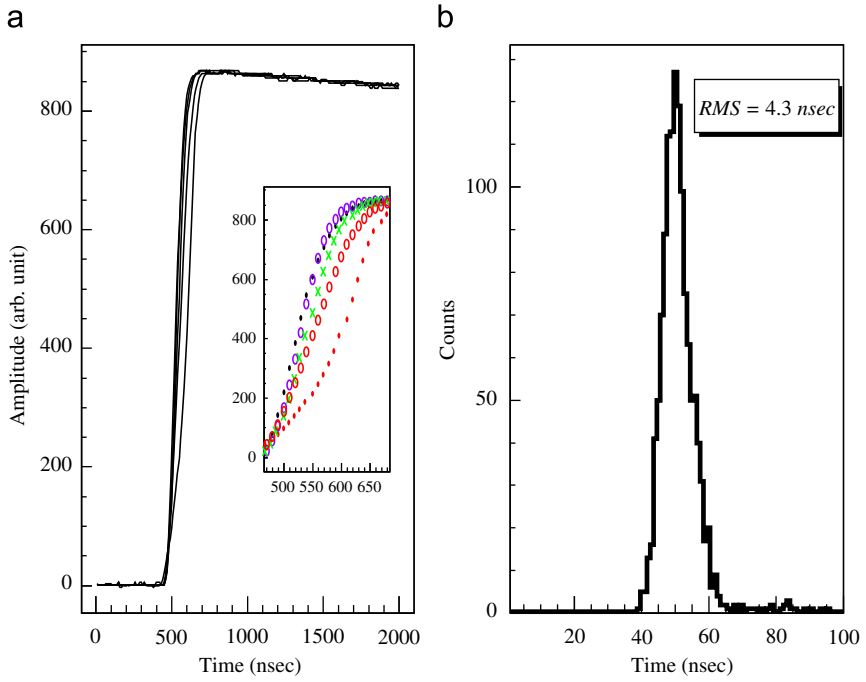

Fig. 3. Traces of the preamplifier pulses of one of the crystals of clover for 1333 keV transition is shown in left panel (a) and its jitter explains higher FWHM for the timing spectrum. The timing spectrum between BaF_2 and one crystal of clover obtained from the offline analysis of preamplifier pulses using digital CFD for ^{60}Co is depicted in (b).

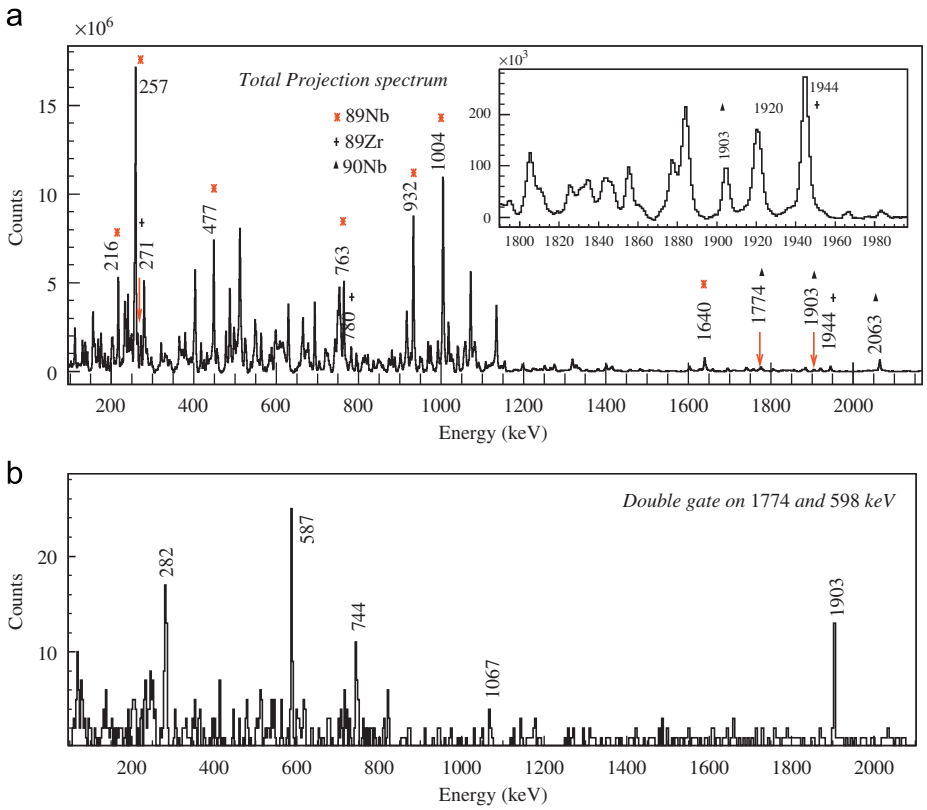

Fig. 4. (a) The total projection spectrum showing the gamma rays of different isotopes produced in the $^{28}Si+^{65}Cu$ reaction. (b) The 1774 keV and 598 keV double gated spectrum depicting the transitions of ^{90}Nb [21].

following equation:

$$FF(i) = \sum_{j=i-(FL-1)}^{i} Trace[j] - \sum_{j=i-(2*FL+FG-1)}^{i-(FL+FG)} Trace[j] \quad (1)$$

The fast length (FL) and fast gap (FG) were kept 100 ns in the present case. Digital CFD for the fast filter of traces were calculated in the offline analysis using Eq. (2) and the zero-crossing time of the CFD response was extracted. This cross-over time was added to the 48-bit FPGA time to get the time of

the event:

$$CFD[i+D] = FF[i+D] - f \times FF[i] \quad (2)$$

The time difference spectrum between the BaF_2 and one of the clover crystal shows a prompt peak in Fig. 3(b) with a *rms* of 4.3 ns. In the present case, we have used a delay of 60 ns and scaling factor (f) of 0.3.

5.3. Two and higher fold gamma–gamma coincidence measurement from time-stamped data

Two fold coincidence between any crystals of the available clovers was set for the current set-up. In the software the firing pattern of a clover was generated from the '*OR*' of its four crystals and this further decides the clover multiplicity in a given event. The addback energies of the different clovers were sorted through the 48-bit time-stamp into two dimensional matrix and three dimensional cube for further analysis. The gated spectra were obtained by symmetrization of the gamma–gamma matrix and gamma–gamma–gamma cube followed by Compton background subtraction using the procedure mentioned in Ref. [28]. First the ^{60}Co data set was used to make the 2d-matrix with a time window of 150 ns. The 1172 and 1333 keV gated spectra were obtained from the matrix to estimate the true and random coincidences. The true to chance coincidence ratio was found to be less than 0.01%.

Further, the present system was tested with several in-beam experiments. Result from one of the experiments using 105 MeV ^{28}Si beam to populate the high spin states of ^{90}Nb using fusion evaporation reaction with Au backed ^{65}Cu target will be presented. The accelerated beam of ^{28}Si was obtained from the 14-UD TIFR-BARC pelletron accelerator facility at TIFR. During the experiment the individual crystal count rate was kept around 5 kHz. With this condition, the 2-fold and 3-fold Compton suppressed clover coincident rates were found to be 15 kHz and 3.5 kHz, respectively. The current DDAQ implementation allowed INGA to take data in excess of five times the previous limited rates. The total projection spectrum is shown in Fig. 4(a) and indicates the production of different isotopes in the present reaction. Some of the strong gamma-ray transitions of ^{89}Nb, ^{89}Zr and ^{90}Nb isotopes are indicated in the total projection. For the coincidence analysis gamma cube was generated with a time coincidence window of 150 ns. The 1774 and 598 keV double gated spectrum shown in Fig. 4(b) indicates 1774–1903–598–587–282–744 keV cascade of ^{90}Nb above the isomeric state shown in the level scheme of Fig. 5 [21].

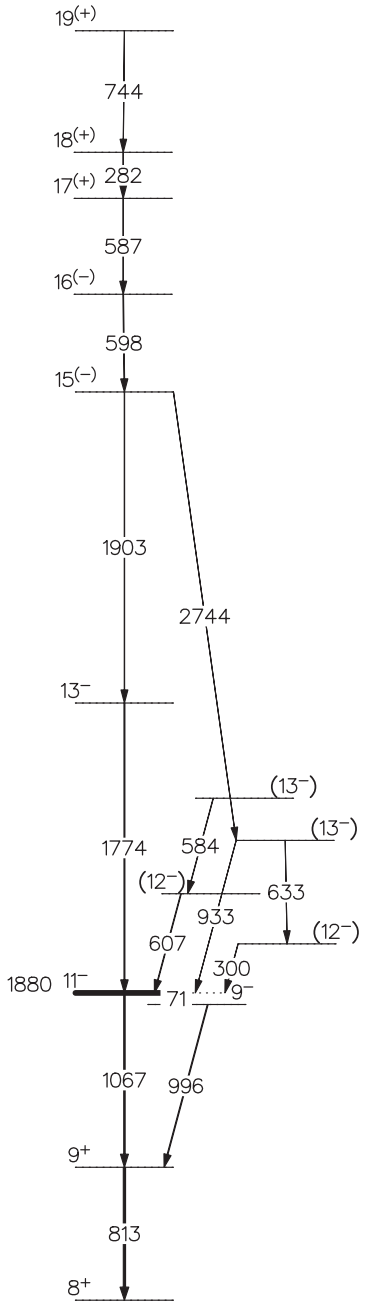

Fig. 5. Partial level scheme of ^{90}Nb [21] relevant for the present discussion.

5.4. Angular distribution measurements in triggerless mode

Measurement of the angular distribution of the strong transitions observed in the in-beam spectrum of ^{28}Si+^{65}Cu reaction at 105 MeV beam energy was carried out using the INGA. The data was collected in a triggerless mode with all the 15 clover detectors distributed in different angles w.r.t. the beam direction. Looking into the timestamp of the events addback spectra for the individual clovers were extracted. The efficiency corrected yield

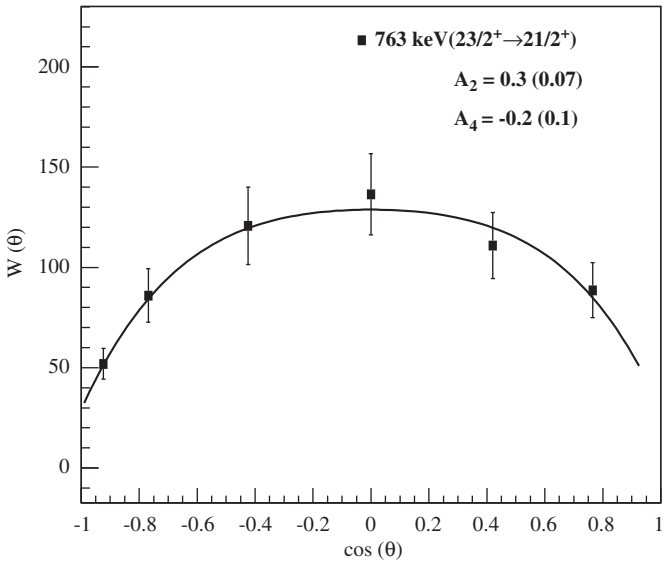

Fig. 6. Angular distribution of 763 keV transition of ^{89}Nb [29]. Here, θ is the angle of the detector w.r.t. the beam direction and $W(\theta)$ is the yield of the gamma-rays in different directions. The solid line presents the fit to the measured data and gives the angular distribution coefficients A_2 and A_4.

of 763 keV transition of ^{89}Nb is shown in Fig. 6. The angular distribution plot suggest a stretched $\Delta I = 1$ nature for 763 keV $(23/2^+ \rightarrow 21/2^+)$ transition of ^{89}Nb isotope in accordance with the previous measurement [29]. During the period of the measurement all the crystals of the clover array were counting at a rate of $\sim$5000 Hz each with a total count rate of about 250 kHz. The successful measurement of the angular distribution of transitions indicates a broad potential of the INGA in the triggerless mode along with its large photopeak efficiency. In particular, measurements where singles data are required such as cross-section measurements for nuclear reaction studies and static quadrupole measurements, the present configuration of the INGA along with the DDAQ will be extremely useful due to its higher efficiency and high count rate handling capability.

5.5. Polarization measurement

Clover detectors kept at 90° with respect to the beam line were used for the polarization measurements for the gamma-rays of ^{89}Nb produced in the ^{28}Si+^{65}Cu reaction at beam energy of 105 MeV. For a Compton-polarimeter, polarization asymmetry Δ of the transition is defined as [30]

$$\Delta = \frac{a(E_\gamma)N_\perp - N_\parallel}{a(E_\gamma)N_\perp + N_\parallel} \quad (3)$$

where, $N_\perp(N_\parallel)$ is the number of counts of gamma transitions scattered perpendicular (parallel) to the reaction plane. The difference spectrum $(a(E_\gamma)N_\perp - N_\parallel)$ measured with 90° detectors obtained with gate on 1003 keV is shown in Fig. 7(a). The correction factor $a(E_\gamma)$ is a measure of the perpendicular to parallel scattering asymmetry within the crystals of clover. For the 90° detectors this parameter has been found to be 1.01(1) from the analysis of decay data of the ^{152}Eu radioactive source (see Fig. 7(b)). For linear polarization measurement, two asymmetric matrices corresponding to parallel and perpendicular segments of clover detectors (with respect to the reaction plane) along one axis and the coincident gamma-rays along the another axis were constructed [17]. Then integrated polarization direction correlation (IPDCO) analysis was carried out. A positive value of IPDCO ratio for 932 keV $(17/2^+ \rightarrow 13/2^+)$ transition of ^{89}Nb indicates its

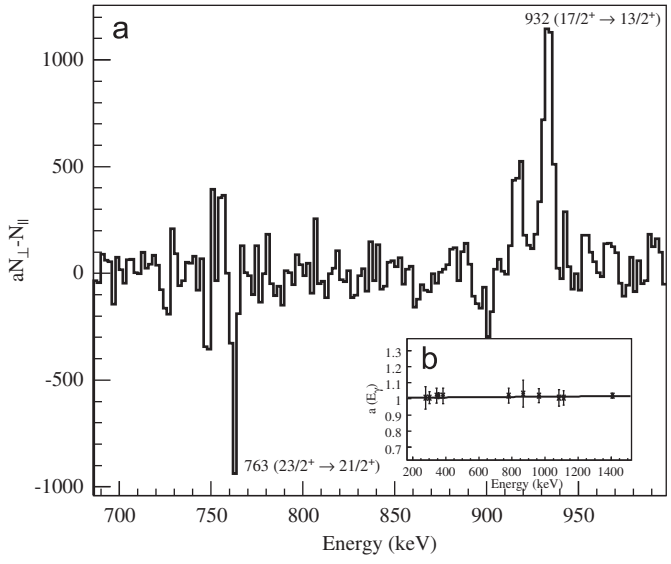

Fig. 7. The difference spectrum generated from the perpendicular and parallel scattering spectra observed in the 90° clovers is shown in (a). Polarization asymmetry of 763 and 932 keV transitions of ^{89}Nb [29] shows their magnetic and electric nature, respectively. Inset (b) shows the asymmetry parameter obtained with the radioactive source.

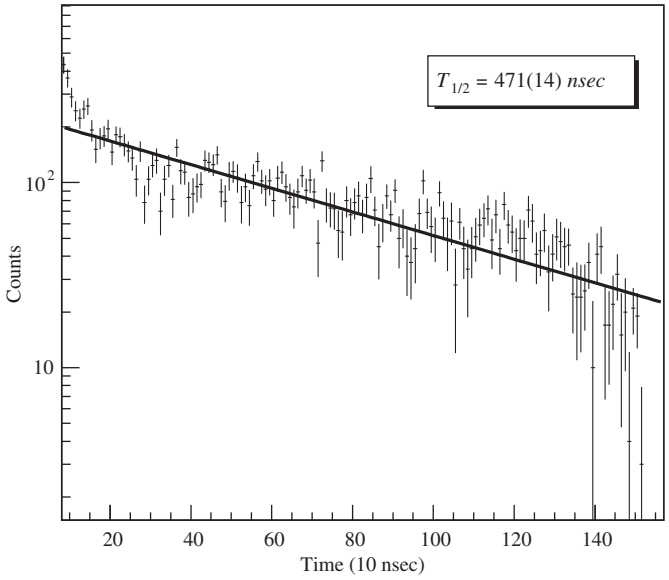

Fig. 8. The time spectrum obtained for the decay of 11^- state in ^{90}Nb at 1880.9 keV excitation energy. This spectrum is generated by measuring at the time difference between 1774 keV and 1067 keV transitions across the isomeric state.

electric nature while negative value for 763 keV $(23/2^+ \rightarrow 21/2^+)$ transition confirms its magnetic nature. These results are in agreement with the level scheme of ^{89}Nb reported in Ref. [29].

5.6. Lifetime measurement based on time-stamp

The 11^- state of ^{90}Nb at 1880.9 keV excitation energy is an isomeric state and decays by 1067.5 and 813.4 keV transitions (see Fig. 8). The half-life of this 11^- state was reported in Ref. [21] to be 470 ± 10 ns by measuring the delayed gamma rays from the isomers at the focal plane of the spectrometer. Time difference spectrum between any two transitions E_1 and E_2 in a cascade can be obtained from the list mode data using the following procedure. Four conditional time spectra ($T_{p1,p2}$,$T_{p1,bg2}$,$T_{bg1,p2}$ and $T_{bg1,bg2}$) need to be generated from the time-stamped data. Here, $T_{p1,p2}$ represents the time difference spectrum obtained with energy gate around the E_1 and E_2 peaks, while $T_{p1,bg2}$ represents the same for energy gate around the E_1 peak and background near E_2 peak. Similarly, the third and fourth spectra are for background-peak and background-background spectra. Then the final time difference spectrum will be given by

$$T(i) = T_{p1,p2}(i) - T_{p1,bg2}(i) - T_{bg1,p2}(i) + T_{bg1,bg2}(i) \quad (4)$$

The decay spectrum obtained from the time difference between the time-stamps of 1774–1067 keV transitions is shown in Fig. 7. The half-life was extracted to be 471 ± 14 ns in the present experiment and is in agreement with the reported lifetime of 470 ± 10 ns in Ref. [21].

6. Summary

A fast digital data acquisition system has been coupled with the Indian National Gamma array consisting of Compton suppressed clover detectors. Several source and in-beam experiments were performed to validate the specifications related to the count rate handling capability, energy resolution, and gain stability. Several experiments were performed using the current set-up to investigate different high spin phenomena and the data sets are under analysis. Angular distribution measurement of 763 keV

gamma ray was carried out in triggerless mode with a total count rate of about 250 kHz for the full array, giving angular distribution coefficients similar to the previous work. Using the time-stamped gamma–gamma coincidence data lifetime of isomeric state of ^{90}Nb was found to be 471(14) ns from the present set-up. Inclusion of a fast timing array consisting of $LaBr_3$(Ce) scintillators with the INGA is planned and their timing properties with the existing DDAQ will be investigated. This will facilitate the lifetime measurements of isomeric states from 1 ns to few μs during the usual gamma–gamma coincidence measurement. Testing of the DDAQ for the light charged particle identification using CsI(Tl) and Si detectors is also planned. The coupling of INGA and its different ancillary detectors to the digital DAQ will improve the overall efficiency and sensitivity of the gamma detector array for nuclear structure and reaction studies. The present work demonstrates that the digital electronics is extremely stable over long data acquisition periods, can easily scale up to large system due to their modular structure, and can run at very high count rates due to its capability to carry out complex real-time triggering to reduce output data rate. Overall the present DDAQ has improved the data recording capability of INGA by a factor of five compared to its previous limited rate due to analogue system.

Acknowledgment

The authors would like to thank the members of INGA Principal Investigating Coordination Committee and the INGA collaboration for making the detectors available. Authors also acknowledge the IUAC group for providing the HV units for the clover detectors and the preamplifiers for BGO detectors. This work was partially funded by the Department of Science and Technology, Government of India (No. IR/S2/PF-03/2003-I). We are thankful to the Pelletron and LINAC staff for providing excellent beam during all experiments of the campaign.

References

[1] I.Y. Lee, Nuclear Physics A 520 (1990) 641c.
[2] C.J. Gross, et al., Nuclear Instruments and Methods in Physics Research Section A 450 (2000) 12.
[3] A. Gadea, et al., European Physical Journal A 20 (2004) 193.
[4] C.W. Beausang, et al., Nuclear Instruments and Methods in Physics Research Section A 452 (2000) 431.
[5] D. Bazzacco, GASP Collaboration, in: International Conference of Nuclear Structure at High Angular Momentum, Ottawa, vol. 2, 1992, 376, AECL 10613.
[6] J. Simpson, et al., Heavy Ion Physics 11 (2000) 159.
[7] H.J. Wollersheim, et al., Nuclear Instruments and Methods in Physics Research Section A 537 (2005) 637.
[8] R.T. Newman, et al., Balkan Physics Letters 182 (1998).
[9] C.E. Svensson, et al., Journal of Physics G: Nuclear and Particle Physics 31 (2005) S1663.
[10] M. Desovich, et al., Nuclear Instruments and Methods in Physics Research Section A 553 (2005) 525.
[11] S. Shimoura, et al., Nuclear Instruments and Methods in Physics Research Section A 525 (2004) 188.
[12] C.W. Beausang, et al., Nuclear Instruments and Methods in Physics Research Section A 313 (1992) 37.
[13] R.K. Bhowmik, in: Proceedings of Fourth International Conference on Fission and Properties of Neutron-Rich Nuclei, World Scientific, 2007, p. 258; H.C. Jain, Pramana 57 (1) (2001) 21; S. Muralithar, et al., Nuclear Instruments and Methods in Physics Research Section A 622 (2010) 281.
[14] R. Palit, H.C. Jain, P.K. Joshi, S. Nagara j, B.V.T. Rao, S.N. Chintalapudi, S.S. Ghugre, Pramana – Journal of Physics 54 (2000) 347.
[15] T. Trivedi, et al., Nuclear Physics A 834 (2010) 72c.
[16] R. Palit, H.C. Jain, P.K. Joshi, J.A. Sheikh, Y. Sun, Physical Review C 63 (2001) 024313.
[17] S. Lakshmi, H.C. Jain, P.K. Joshi, I. Mazumdar, R. Palit, A.K. Jain, S.S. Malik, Nuclear Physics A 761 (2005) 12.
[18] D. Choudhury, et al., Physical Review C 82 (2010) 061308.
[19] S. Sihotra, et al., Physical Review C 78 (2008) 034313.
[20] R. Chakrabarti, et al., Physical Review C 80 (2009) 034326.
[21] A. Chakraborty, et al., Physical Review C 72 (2005) 054309.
[22] H. Tan, et al., in: Nuclear Science Symposium Conference Record, NSS 08, IEEE, 2008, p. 3196.
[23] W. Hennig, H. Tan, M. Walby, P. Grudberg, A. Fallu-Labruyere, W.K. Warburton, C. Vaman, K. Starosta, D. Miller, Nuclear Instruments and Methods in Physics Research Section B 261 (2007) 1000.
[24] P.K. Joshi, et al., Nuclear Instruments and Methods in Physics Research 399 (1997) 51.
[25] P.J. Nolan, F.A. Beck, D.B. Fossan, Annual Review of Nuclear and Particle Science 45 (1994) 561.
[26] R. Palit, AIP Conference Proceedings 1336 (2011) 573.
[27] V.V. Parkar, et al., Physical Review C 82 (2010) 054601.
[28] D.C. Radford, Nuclear Instruments and Methods in Physics Research Section A 361 (1995) 306.
[29] A. Bodeker, K.P. Lieb, C.J. Gross, M.K. Kabadiyski, D. Rudolph, M. Weiszflog, J. Eberth, H. Grawe, J. Heese, K.-H. Maier, Physical Review C 48 (1993) 1617.
[30] K. Starosta, et al., Nuclear Instruments and Methods in Physics Research Section A 423 (1999) 16.